

PathMLP: Smooth Path Towards High-order Homophily

Chenxuan Xie*
Institute of Cyberspace Security
Zhejiang University of Technology
hello.craboss@gmail.com

Jiajun Zhou*[†]
Institute of Cyberspace Security
Zhejiang University of Technology
jjzhou@zjut.edu.cn

Shengbo Gong
Institute of Cyberspace Security
Zhejiang University of Technology
jshmhsb@gmail.com

Jiacheng Wan
Institute of Cyberspace Security
Zhejiang University of Technology
ete_bosh@outlook.com

Jiaxu Qian
Institute of Cyberspace Security
Zhejiang University of Technology
q1anjiaxu001@gmail.com

Shanqing Yu
Institute of Cyberspace Security
Zhejiang University of Technology
yushanqing@zjut.edu.cn

Qi Xuan
Institute of Cyberspace Security
Zhejiang University of Technology
xuanqi@zjut.edu.cn

Xiaoniu Yang
Institute of Cyberspace Security
Zhejiang University of Technology
yxn2117@126.com

ABSTRACT

Real-world graphs exhibit increasing heterophily, where nodes no longer tend to be connected to nodes with the same label, challenging the homophily assumption of classical graph neural networks (GNNs) and impeding their performance. Intriguingly, we observe that certain high-order information on heterophilous data exhibits high homophily, which motivates us to involve high-order information in node representation learning. However, common practices in GNNs to acquire high-order information mainly through increasing model depth and altering message-passing mechanisms, which, albeit effective to a certain extent, suffer from three shortcomings: 1) over-smoothing due to excessive model depth and propagation times; 2) high-order information is not fully utilized; 3) low computational efficiency. In this regard, we design a similarity-based path sampling strategy to capture smooth paths containing high-order homophily. Then we propose a lightweight model based on multi-layer perceptrons (MLP), named PathMLP, which can encode messages carried by paths via simple transformation and concatenation operations, and effectively learn node representations in heterophilous graphs through adaptive path aggregation. Extensive experiments demonstrate that our method outperforms baselines on 16 out of 20 datasets, underlining its effectiveness and superiority in alleviating the heterophily problem. In addition, our method is immune to over-smoothing and has high computational efficiency.

CCS CONCEPTS

• **Computing methodologies** → **Neural networks.**

*Both authors contributed equally to this research.

[†]Jiajun Zhou is the corresponding author.

Permission to make digital or hard copies of all or part of this work for personal or classroom use is granted without fee provided that copies are not made or distributed for profit or commercial advantage and that copies bear this notice and the full citation on the first page. Copyrights for components of this work owned by others than ACM must be honored. Abstracting with credit is permitted. To copy otherwise, or republish, to post on servers or to redistribute to lists, requires prior specific permission and/or a fee. Request permissions from [permissions@acm.org](https://permissions.acm.org).
Conference acronym 'XX, June 03–05, 2018, Woodstock, NY

© 2018 Association for Computing Machinery.
ACM ISBN 978-1-4503-XXXX-X/18/06...\$15.00
<https://doi.org/XXXXXXXX.XXXXXXX>

KEYWORDS

graph neural network, heterophily, homophily, node classification

ACM Reference Format:

Chenxuan Xie, Jiajun Zhou, Shengbo Gong, Jiacheng Wan, Jiaxu Qian, Shanqing Yu, Qi Xuan, and Xiaoniu Yang. 2018. PathMLP: Smooth Path Towards High-order Homophily. In *Proceedings of Make sure to enter the correct conference title from your rights confirmation email (Conference acronym 'XX)*. ACM, New York, NY, USA, 10 pages. <https://doi.org/XXXXXXXX.XXXXXXX>

1 INTRODUCTION

Graphs are used to model various interaction scenarios in the real world, such as social networks [9], recommendation systems [35], financial transactions [38], etc. Based on this, graph neural networks (GNNs) have been widely explored and developed in order to efficiently process non-Euclidean graph structured data. GNNs propagate, aggregate, and transform node and edge features via message-passing mechanisms to learn node and edge representations, and have achieved excellent performance in various tasks such as node classification and link prediction.

Classical GNNs [12, 14, 33] obey homophily assumption, i.e., nodes with similar features or the same labels are more likely to be connected. The phenomenon of graph homophily is markedly exemplified in social networks and citation networks. For example, people in social networks are more likely to make friends with those sharing similar interests; in citation networks, researchers are more likely to cite papers within their field [23]. However, real-world graphs are exhibiting increasing heterophily, where connected nodes possess dissimilar features or labels. For example, fraudulent accounts in financial networks generally interact with a large number of victim (normal) accounts; there is cross-disciplinary interactions in scientific collaboration networks [5]. Such phenomena challenge the homophily assumption of classical GNNs, hinder their performance, and raises the *heterophily problem*.

Existing studies [32, 41] argue that low-order information surrounding the target node contains more noise in heterophilous scenarios. Unfiltered aggregation of low-order information can severely interfere with the representations of node. To confirm this, we count the average homophily of different orders in homophilous

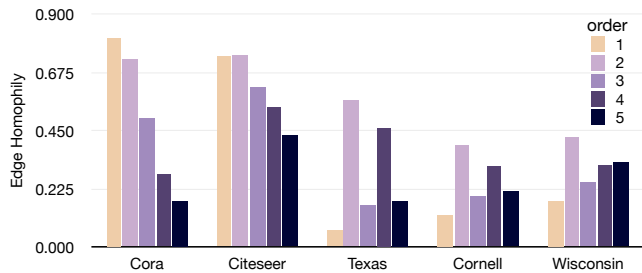


Figure 1: Edge homophily in different order.

and heterophilous datasets, as shown in Fig. 1, from which we can observe that higher-order information in heterophilous graphs (e.g., *Texas*, *Cornell* and *Wisconsin*) indeed exhibits stronger homophily than lower-order information. This inspires us to utilize higher-order information to alleviate the heterophily problem.

Some classical GNNs such as GAT [33] first consider the importance of different neighbors, and then stack convolutional layers to obtain higher-order information. Although this approach can explicitly reduce the impact of heterophilous noise, the layer stacking leads to the over-smoothing problem, i.e., features of different nodes become indistinguishable as the number of convolutional layers increases, thus diminishing model performance. Other approaches introduce high-order message-passing mechanisms, i.e., using high-order information during message passing. H2GCN [40] and Mixhop [1] aggregate information from first-order and second-order neighbors during message passing, and GPRGNN [7] learns a generalized PageRanks (GPR) weight to adaptively aggregate node features and high-order information after multiple propagation. However, the former models still obtain high-order information by stacking, failing to circumvent the over-smoothing problem caused by excessive model depth. The latter claims they obtain the high-order information by self-multiplication of adjacent matrix, but the weight of high-order nodes has been overly averaged, limiting their contribution to the target nodes.

Path-based approaches believe that node behavior preferences are implied in path information, and realize message aggregation by path sampling and using recurrent neural network (RNN)-like models to extract features from paths. For example, RAWGNN [13] uses Node2Vec [11] to simulate breadth-first search (BFS) and depth-first search (DFS), attempting to obtain homophilous and heterophilous information. PathNet [30] employs the entropy increase idea to guide path sampling and obtain different preference paths for different nodes. However, these approaches have obvious drawbacks: 1) unreasonable sampling strategies. Both sampling strategies tend to capture structural information around target nodes rather than homophilous or heterophilous information, failing to effectively guide node representation learning in heterophilous scenarios; 2) inefficiency. Each sampled path needs to be processed by RNN-like models, leading to huge computational cost.

To alleviate the heterophilous problem while avoiding the aforementioned drawbacks, we propose a PathMLP method. Specifically, we first design a similarity-based path sampling strategy to obtain smooth paths with high-order homophily for target nodes. Then,

the PathMLP model can encode path information through concatenation and transformation operations, and generate highly expressive node representations in heterophilous scenarios through adaptive message aggregation. We conduct extensive experiments on five homophilous datasets and five heterophilous datasets to evaluate our methods, and the results show that our methods achieve the best performance on 16 out of 20 datasets, verifying its effectiveness and superiority in alleviating the heterophily problem. Additionally, our method can obtain higher-order information through path sampling without relying on model stacking, effectively avoiding the over-smoothing problem. Meanwhile, in our framework, all feature extraction, propagation, aggregation, and transformation are implemented through MLP only, making PathMLP highly computationally efficient. Finally, our contributions can be summarized as follows:

- To the best of our knowledge, we are the first to propose a path sampling strategy based on feature similarity to obtain high-order information for alleviating heterophily problem.
- We implement a PathMLP model via MLP only, which can efficiently encode path features for node classification in heterophilous scenarios through adaptive message aggregation.
- Extensive experiments on 20 benchmarks verify the effectiveness and superiority of PathMLP in alleviating heterophily problems. Meanwhile, PathMLP is not disturbed by the over-smoothing problem and has high computational efficiency.

2 PRELIMINARIES

2.1 Notations

An attributed graph can be represented as $G = (V, E, X)$, where V and E are node set and edge set respectively, $X \in \mathbb{R}^{|V| \times f}$ is node feature matrix. Here we use $|V|$, $|E|$ and f to denote the number of nodes and edges, and the dimension of node feature. The structure elements (V, E) can also be denoted as an adjacency matrix $A \in \mathbb{R}^{|V| \times |V|}$ that encodes pairwise connections between the nodes, whose entry $A_{ij} = 1$ if there exists an edge between v_i and v_j , and $A_{ij} = 0$ otherwise. Based on adjacency matrix, we can define the re-normalized affinity matrix as $\tilde{A}_{\text{sym}} = \tilde{D}^{-1/2} \tilde{A} \tilde{D}^{-1/2}$, where $\tilde{A} = A + I$ and $\tilde{D} = D + I$. Finally we define a path that starts from node v_i and is within its h -order neighborhood:

$$p_i = [v_i, v_1, v_2, \dots, v_j, \dots, v_d] \quad (1)$$

with $v_j \in \mathcal{N}_i^h \cup \{v_i\}$, $1 \leq j \leq d$

where \mathcal{N}_i^h is the neighbor set within h -order neighborhood of v_i .

2.2 Homophily

Homophily refers to the fact that nodes with similar attributes are more likely to be connected, or furthermore, nodes are more likely to be connected to nodes with the same label. This phenomenon is reflected in many real social networks and information networks.

2.2.1 Edge Homophily. Edge homophily [40] defines the proportion of edges that connect two nodes of the same class (i.e., intra-class edges) in a graph:

$$H_{\text{edge}}(G) = \frac{|\{(v_i, v_j) \in E \mid y_i = y_j\}|}{|E|} \quad (2)$$

where y is the label of node. The lower $H_{\text{edge}}(G)$ implies more inter-class edges in the graph, i.e., stronger heterophily.

2.2.2 Adjusted Homophily. Edge homophily metric cannot measure the homophily of imbalanced datasets well, as it tends to be affected by majority class nodes. To address this, adjusted homophily [25] has been proposed, which further considers the relationship between edge and node degrees based on edge homophily, and can better measure the homophily of imbalanced datasets.

$$H_{\text{adj}}(G) = \frac{H_{\text{edge}} - \sum_{c=1}^C D_c^2 / (2|E|)^2}{1 - \sum_{c=1}^C D_c^2 / (2|E|)^2} \quad (3)$$

where D_c denotes the sum of the degrees of all nodes belonging to class c , and C is the number of node classes.

In this paper, we use edge homophily to measure the all datasets except imbalanced datasets *Questions* and *Tolokers*.

3 RELATED WORK

Previous studies have extensively explored the graph heterophily problem, and we categorize some existing studies into four classes: based on high-order information [1, 7, 40], graph structural information [16, 17, 21], paths [13, 30], and others [3, 10, 19, 24, 41].

High-order information is considered beneficial for alleviating heterophily in graphs, hence some methods have designed high-order message-passing mechanisms to exploit higher-order information. H2GCN [40] and Mixhop [1] incorporate both first- and second-order neighborhood information during message-passing. GPRGNN [7] learns GPR weights to adaptively aggregate node features and high-order information. Several other studies tend to focus on the graph structural information. LINKX [17] combines the adjacency matrix with MLP and node features for node classification. GloGNN [16] use the adjacency matrix like LINKX and learns correlations between nodes to aggregate information from global nodes. FSGNN [21] tries to select features for propagation using the adjacency matrix, investigating the impact of features of different orders on performance.

Moreover, a considerable number of studies consider that path information can effectively capture the behavior patterns of nodes, aiding in characterizing node features in heterophilous scenarios. GeniePath [18] proposes adaptive breadth and depth functions to select important nodes in first-order and higher-order neighbors. It aggregates neighbors like GAT to get breadth information and then adopts RNN-like architecture with adaptive depth to process nodes from different orders. SPAGAN [37] exploits the shortest path to explore latent graph structure and conducts path-based attention to achieve a more effective aggregation. PathNet [30] use maximal entropy-based random walk to capture heterophily of neighbors and retain useful structural information. RAWGNN [13] utilizes Node2Vec [11] to simulate BFS and DFS to capture homophily and heterophily information respectively. However, the sampling strategies of these methods can only capture the structural features around nodes, and their computational efficiency is also constrained by RNN-like aggregators.

Other methods aim to alleviate the heterophily problem from spectral or spatial domain. FAGCN [3] adaptively integrates low-frequency and high-frequency signals to learn node representations.

ACMGCN [19] adaptively aggregates the three channels of high-pass, low-pass, and identity to extract richer information and can adapt to more different heterophilous scenarios. Geom-GCN [24] updates node features by aggregating structural neighborhoods in the continuous latent space behind the network. SNGNN [41] replaces the edge weights with similarity of nodes and utilizes a topk-based strategy to select useful neighbors. GGCN [36] learns new signed edge weight by structure-based edge correction and feature-based edge correction to adjust the influence of neighbors. NHGCN [10] proposes a new metric, named neighborhood homophily, to guide a multi-channel neighbor aggregation.

4 METHOD

In this section, we will detail our PathMLP framework, including the similarity-based path sampling and the model. Fig. 2 illustrates the overall framework.

4.1 Path Sampling

To address the weaknesses of existing path sampling strategies, we propose a new feature similarity-based sampling strategy, which progressively acquires paths starting from target nodes, guided by hop-by-hop similarity. This strategy ensures the features along paths will not deviate from start nodes excessively. The smoothness of feature is proved beneficial to node representation [41].

Our path sampling proceeds as follows: For a node path $p_i = [v_i, v_1, v_2, \dots, v_j, \dots, v_d]$ of length $d + 1$, the head node ($j = 0$) is the target node v_i . The second node ($j = 1$, denoted as v_1) is one of the two most similar neighbors to v_i . The third node ($j = 2$, denoted as v_2) is one of the three most similar neighbors to v_1 , and so forth; the fifth node ($j = 4$, denoted as v_4) is one of the five most similar neighbors to v_3 . Starting from the sixth node ($j = 5$, denoted as v_5), each subsequent node ($j \geq 5$) is the most similar neighbor to the previous one. The sampling process stops when the path reaches the specified length ($d + 1$). From the above process, when d is $\{1, 2, 3, 4, 5, 6, \dots\}$, we can respectively obtain $\{2, 6, 24, 120, 120, 120, \dots\}$ candidate paths. As can be observed, when the length of the path to be sampled is greater than 5, the number of candidate paths no longer increases, preventing exponential growth in the number of candidate paths due to too large sampling parameters. Finally, nodes on the path can be formally represented as follows:

$$p_i[j] \in \begin{cases} \{v_i\} & \text{for } j = 0 \\ \text{top}(j+1)(\mathcal{N}_i^1 | \mathbf{x}_i^\top \cdot \mathbf{x}_j) & \text{for } j = 1 \\ \text{top}(j+1)(\mathcal{N}_{j-1}^1 | \mathbf{x}_{j-1}^\top \cdot \mathbf{x}_j) & \text{for } 2 \leq j \leq 4 \\ \text{top}(1)(\mathcal{N}_{j-1}^1 | \mathbf{x}_{j-1}^\top \cdot \mathbf{x}_j) & \text{for } j \geq 5 \end{cases} \quad (4)$$

where \mathbf{x}_j is the feature of node $v_j \in \mathcal{N}_i^1$ or \mathcal{N}_{j-1}^1 , $\text{top}(j)(\mathcal{N} | \text{func})$ means to get the largest j elements from the set \mathcal{N} according to the similarity defined by func . Note that we use inner product here to calculate the node similarity.

After similarity-based path sampling, each target node obtains a set of candidate paths, where the possible number of paths is $\{2, 6, 24, 120\}$, determined by the path length. Considering that using too many candidate paths for message aggregation at the target nodes poses the over-squashing problem [2] when the paths are

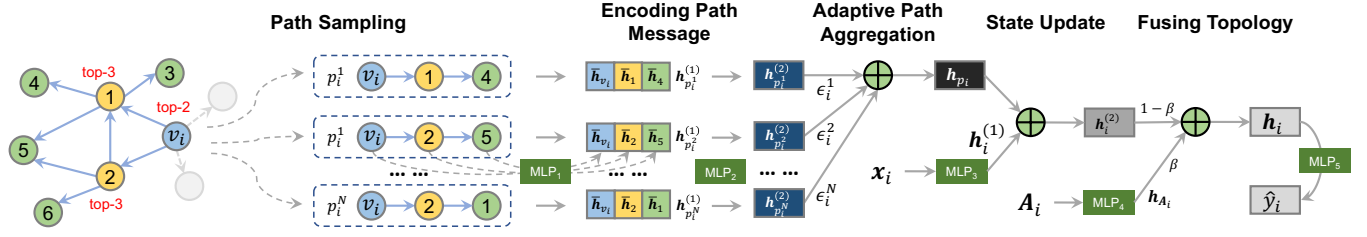


Figure 2: Illustration of the PathMLP framework.

long, we randomly sample a number of candidate paths (parameterized by N) to participate in the subsequent message aggregation.

4.2 Model

These candidate paths are subsequently engaged in message aggregation, updating the features of the target nodes. Previous studies [13, 30] utilize RNN-like models as aggregators to process paths, which encounters two issues: 1) the features of all nodes on the path are squeezed into the target node, causing the over-squashing inevitably; 2) each sequence needs to be processed separately with RNN-like models, leading to a huge computational cost.

4.2.1 PathMLP. To address the aforementioned issues, in this paper, we first use only MLPs as the aggregators for path to node message aggregation and propose a PathMLP model. It can encode the message carried by the paths through simple concatenation operations, and adaptively aggregates the paths start from one node to obtain its representation.

Step 1: Encoding Path Message. After path sampling, each node v_i obtains N paths $\{p_i^k \mid k = 1, \dots, N\}$, containing high-order homophilous information of the target node. For each path p_i^k of the target node v_i , we encode its information. Specifically, we first encode each node on the path using a linear transformation and non-linear activation:

$$\bar{h}_v = \sigma(\text{MLP}_1(x_v)) \quad \text{for } v \in p_i^k \quad (5)$$

where MLP_1 is parameterized by $\mathbf{W}_1 \in \mathbb{R}^{f \times f'}$, and σ is the activation function. The path features are obtained by concatenating the features of the nodes on the path:

$$\mathbf{h}_{p_i^k}^{(1)} = \parallel_{v \in p_i^k} \bar{h}_v \quad (6)$$

To improve the expressiveness of the path features, we again encode the path features using linear transformation and nonlinear activation:

$$\mathbf{h}_{p_i^k}^{(2)} = \sigma\left(\text{MLP}_2\left(\mathbf{h}_{p_i^k}^{(1)}\right)\right) \quad (7)$$

where MLP_2 is parameterized by $\mathbf{W}_2 \in \mathbb{R}^{(1+d) \cdot f' \times f_h}$, and f_h is the hidden dimension.

Step 2: Adaptive Path Aggregation. Different paths of the target node capture different high-order features. To better learn the representations of the target node, path message are generated here

by adaptively aggregating different path features.

$$\mathbf{h}_{p_i} = \sum_{k=1}^N \epsilon_i^k \cdot \mathbf{h}_{p_i^k}^{(2)} \quad \text{with } \sum_{k=1}^N \epsilon_i^k = 1 \quad (8)$$

where ϵ_i^k is the learnable weight for the k -th path of node v_i .

Step 3: State Update. After obtaining the path message for target node, PathMLP updates its state by adding the path message to the original feature of the target node:

$$\begin{aligned} \mathbf{h}_i^{(1)} &= \sigma(\text{MLP}_3(x_i)) \\ \mathbf{h}_i^{(2)} &= \mathbf{h}_i^{(1)} + \mathbf{h}_{p_i} \end{aligned} \quad (9)$$

where MLP_3 is parameterized by $\mathbf{W}_3 \in \mathbb{R}^{f \times f_h}$.

Step 4: Fusing Topological Information. Topological information is crucial for characterizing node features. To alleviate the shortcomings of MLP in capturing topological information, we further incorporate topological information into the representation of target nodes in a controlled manner:

$$\begin{aligned} \mathbf{h}_{A_i} &= \sigma(\text{MLP}_4(A_i)) \\ \mathbf{h}_i &= \beta \cdot \mathbf{h}_{A_i} + (1 - \beta) \cdot \mathbf{h}_i^{(2)} \end{aligned} \quad (10)$$

where MLP_4 is parameterized by $\mathbf{W}_4 \in \mathbb{R}^{|V| \times f_h}$, and $\beta \in [0, 1]$ is a scalar weight to balance node feature and topological information.

Step 5: Model Training. We employ cross-entropy as the classification loss:

$$\begin{aligned} \hat{\mathbf{y}}_i &= \text{Softmax}(\text{MLP}_5(\mathbf{h}_i)) \\ \mathcal{L} &= -\frac{1}{|V_{\text{train}}|} \sum_{v_i \in V_{\text{train}}} \mathbf{y}_i \cdot \log(\hat{\mathbf{y}}_i) \end{aligned} \quad (11)$$

where MLP_5 is parameterized by $\mathbf{W}_5 \in \mathbb{R}^{f_h \times C}$, C is the number of node classes, and \mathbf{y}_i is the one-hot label of v_i . Algorithm 1 shows the process of training PathMLP.

4.2.2 Variant based on Feature Augmentation: PathMLP+. Previous studies [15, 34] pointed out that, as a special case of Laplacian smoothing, the GCN-like graph convolution operation improve the smoothness between the target node and its surrounding neighbors by mixing their features. This indicates that simply multiplying the raw features and the adjacent matrix can also provide the smoothness we need to some extent. Thus we introduce graph feature augmentation [39] based on the GCN-like graph convolution to further improve the smoothness of the path features. Specifically, we first apply the GCN-like convolution to the raw features of nodes,

then concatenate the smoothed features with the raw features to achieve feature augmentation.

$$\tilde{x}_v = x_v \parallel \tilde{A}_{\text{sym}}^m x_v \quad (12)$$

where \tilde{x}_v is the augmented node feature, and $m \in \{1, 2\}$.

Algorithm 1: Training PathMLP.

Input: Graph $G = (V, E, X)$, length parameter of path d , number of paths N .
 /* Sampling paths */
 1 **for** $v_i \in K$ **do**
 2 Get all candidate paths for v_i via Eq. (4);
 3 Sampling N paths for v_i : $\{p_i^k \mid k = 1, \dots, N\}$;
 4 **end**
 /* Training model */
 5 Train PathMLP via Eq. (5) - (11);

5 EXPERIMENTS

5.1 Dataset

Current heterophilous benchmarks mainly include *Chameleon*, *Squirrel*, *Texas*, *Cornell*, *Wisconsin*, and *Actor*. In recent years, most studies have focused on improving the performance of models used to alleviate heterophily problem on these benchmarks, while neglecting to consider the benchmarks themselves. Platonov et al. [26] found serious data leakage issues in *Chameleon* and *Squirrel*, where some nodes exhibit identical adjacency relationships and labels. Additionally, we argue that the scale of some benchmarks such as *Texas*, *Cornell* and *Wisconsin* is rather small, which makes them susceptible to variations in the results based on different data splitting settings. In this regard, we collect benchmarks used in current studies on the heterophily problem and divided them into two groups:

- **Normal Group:** This group comprises datasets that are free from data leakage issues, of normal scale, and have undergone de-duplication. Specifically, they are *Cora*, *Citeseer*, *Pubmed*, *Cora-full*, *Actor*, *Chameleon-f*, *Squirrel-f*, *Tolokers*, *Penn94*, and *Electronics*. Notably, *Chameleon-f* and *Squirrel-f* are the de-duplicated versions of *Chameleon* and *Squirrel*.
- **Anomaly Group:** This group comprises datasets that suffer from data leakage issues or are of smaller scale. Specifically, they are *Chameleon*, *Squirrel*, *Texas*, *Cornell*, *Wisconsin*, *NBA*, *Questions*, *Amazon-ratings*, and *BGP*. Remarkably, although Platonov et al. pointed out the data leakage issues in some existing benchmarks and proposed some new benchmarks, they did not seem to check these new benchmarks such as *Questions* and *Amazon-ratings*, which also have data leakage. Please refer to Appendix A.3 for data leakage detection.

For all datasets, we consider datasets with graph homophily (the average homophily of all nodes) below 0.5 as heterophilous graphs. For detailed descriptions of these benchmarks and their data leakage status, please refer to Appendix A.

5.2 Baselines

We compare our PathMLP and PathMLP+ with 14 various baselines, which can be categorized into five groups: 1) Classical GNNs:

MLP [27], GCN [14], GraphSAGE [12] and GAT [33]; 2) High-order methods: GPRGNN [7] and H2GCN [40]; 3) Path-based methods: RAWGNN [13]; 4) Methods using both node feature and graph structure: LINKX [17], FSGNN [21], GloGNN [16]; 5) Other methods: FAGCN [3], ACMGCN [19], GCNII [6], SNGNN [41].

5.3 Settings

For most datasets, we use random splitting (48%/32%/20% for training/validation/testing) which is different from [24]. For *Tolokers*, *Questions*, *Roman-empire* and *Amazon-ratings*, we use the splitting setting (50%/25%/25% for training/validation/testing) according to [26]. We evaluate all methods with 10 runs and report the average test accuracies (or AUC for *Questions* and *Tolokers*). We set the optimizer to Adam, the maximum epochs to 500 with 100 epochs patience for early stopping, and the hidden dimension f_h to 64. The search spaces of weight decay, learning rate and dropout rate are shared by all methods. Refer to the Appendix B for details on the hyper-parameter settings of our methods and baselines.

5.4 Node Classification

We evaluate the performance of our PathMLP and its variants via node classification tasks on 20 benchmarks. For fair comparison, we measure the expressive power of different models based on their performance on the normal group.

Table 1 presents the node classification results of all methods on the normal group. We can see that our methods achieve the best performance on 3 out of 5 homophilous graphs (*Citeseer*, *Cora-full*, and *Electronics*) and on 5 out of 6 heterophilous graphs (except *Roman-empire*). Moreover, PathMLP and PathMLP+ achieve the top two average performance rankings, demonstrating the effectiveness and superiority of our methods across datasets with varying levels of homophily. Notably, PathMLP+ outperforms PathMLP on most datasets, indicating the effectiveness of our feature augmentation. In addition, classical GNNs, for they comply with the homophily assumption, perform poorly on heterophilous graphs, while other models exhibit fluctuating performance across different datasets.

Table 2 presents the node classification results of all methods on the anomaly group. We observe that our methods can achieve the optimal performance on most datasets and get the top two average performance rankings. We first focus on datasets with data leakage problems (*Chameleon*, *Squirrel*, *Questions*, *Amazon-ratings* and *BGP*), where nodes with identical neighbors and labels are distributed among the training, validation and testing sets. For these datasets, methods that use graph structure information (LINKX, GloGNN, FSGNN and our models) will learn shortcuts, i.e., use graph structure information (\mathcal{A}) to match the neighbors of the target node without using node features. In particular, LINKX, as a simple model, can achieve better performance on these datasets than models specifically designed for heterophilous graphs.

For these small-scale datasets (*Texas*, *Cornell*, *Wisconsin*, and *NBA*), our methods achieve superior performance with high stability, as evidenced by lower standard deviations. Meanwhile, MLP performs well on *Texas*, *Cornell* and *Wisconsin*, beating almost all other baselines, implying that nodes in these three datasets tend to rely on their own features.

Table 1: Node classification results on real-world benchmarks (Normal Group). Boldface letters are used to mark the best results while underlined letters are used to mark the second best results. † represent the homophily is evaluated by adjusted homophily.

	Cora	Citeseer	Pubmed	Cora-fill	Electronics	Actor	Chamenlon-f	Squirrel-f	Tolokers	Roman-empire	Penn94	Avg. Rank
Homophily	0.81	0.74	0.80	0.57	0.58	0.22	0.25	0.22	0.09	0.05†	0.47	
#Nodes	2708	3327	19717	19793	42318	7600	890	2223	11758	22662	41554	
#Edges	10556	9104	88648	126842	129430	30019	13584	65718	1038000	65854	2724458	
#Features	1433	3703	500	8710	8669	932	2325	2089	10	300	4814	
#Classes	7	6	3	70	167	5	5	5	2	2	3	
MLP	76.32 ± 0.99	72.56 ± 1.32	88.06 ± 0.4	60.12 ± 0.92	76.84 ± 0.39	37.14 ± 1.06	33.31 ± 2.32	34.47 ± 3.09	53.18 ± 6.35	65.98 ± 0.43	75.18 ± 0.35	13.4
GCN	88.41 ± 0.77	76.68 ± 1.00	88.19 ± 0.48	71.09 ± 0.62	65.52 ± 0.43	30.65 ± 1.06	41.85 ± 3.22	33.89 ± 2.61	70.34 ± 1.64	50.76 ± 0.46	80.45 ± 0.27	11.9
GraphSAGE	87.93 ± 0.94	76.74 ± 1.05	89.03 ± 0.34	71.37 ± 0.52	76.77 ± 0.27	37.60 ± 0.95	44.94 ± 3.67	36.61 ± 3.06	82.37 ± 0.64	77.77 ± 0.49	OOM	8.0
GAT	87.78 ± 1.17	76.38 ± 1.23	87.80 ± 0.29	69.21 ± 0.52	65.82 ± 0.39	30.58 ± 1.18	43.31 ± 3.42	36.27 ± 2.12	79.93 ± 0.77	57.34 ± 1.81	78.10 ± 1.28	12.7
GPRGNN	88.83 ± 1.13	<u>77.46 ± 0.77</u>	89.55 ± 0.52	<u>71.78 ± 0.69</u>	70.22 ± 0.36	36.89 ± 0.83	44.27 ± 5.23	40.58 ± 2.00	73.84 ± 1.40	67.72 ± 0.63	84.34 ± 0.29	6.9
H2GCN*	88.43 ± 1.50	77.35 ± 1.04	89.67 ± 0.42	70.98 ± 0.76	76.89 ± 0.47	37.27 ± 1.27	43.09 ± 3.85	40.07 ± 2.73	81.34 ± 1.16	79.47 ± 0.43	75.91 ± 0.44	6.5
RAWGNN	86.19 ± 1.22	75.79 ± 1.23	89.12 ± 0.47	65.75 ± 0.98	73.45 ± 0.50	37.30 ± 0.77	46.24 ± 4.07	37.44 ± 2.35	80.56 ± 0.73	82.19 ± 0.33	74.90 ± 0.52	9.3
LINKX	83.33 ± 1.86	72.63 ± 0.80	86.99 ± 0.64	66.68 ± 0.96	75.01 ± 0.44	31.17 ± 0.61	44.94 ± 3.08	38.40 ± 3.54	77.55 ± 0.80	61.36 ± 0.60	84.97 ± 0.46	11.2
GloGNN*	85.16 ± 1.76	74.84 ± 1.35	89.35 ± 0.54	66.10 ± 1.10	<u>76.93 ± 0.36</u>	37.30 ± 1.41	41.46 ± 3.89	37.66 ± 2.12	58.74 ± 13.41	66.46 ± 0.41	85.63 ± 0.27	9.9
FSGNN	88.39 ± 1.16	77.16 ± 0.89	89.94 ± 0.55	60.12 ± 0.92	OOM	37.14 ± 1.06	45.79 ± 3.31	38.25 ± 2.62	83.87 ± 0.98	79.76 ± 0.41	83.87 ± 0.98	6.8
FAGCN	88.21 ± 1.20	76.63 ± 1.13	89.89 ± 0.36	71.61 ± 0.54	73.42 ± 1.61	37.59 ± 0.95	45.28 ± 4.33	<u>41.05 ± 2.67</u>	81.38 ± 1.34	75.83 ± 0.35	79.01 ± 1.09	6.5
ACMGCN	88.50 ± 0.97	76.72 ± 0.70	<u>90.03 ± 0.44</u>	71.59 ± 0.78	76.91 ± 0.27	36.89 ± 1.13	43.99 ± 2.02	36.58 ± 2.75	83.52 ± 0.87	79.57 ± 0.35	83.01 ± 0.46	6.1
GCNII*	87.84 ± 1.07	77.25 ± 0.92	90.21 ± 0.42	70.57 ± 0.98	76.73 ± 0.35	<u>37.67 ± 1.10</u>	44.66 ± 5.40	38.56 ± 2.88	83.71 ± 1.86	78.85 ± 0.54	75.20 ± 0.33	6.4
SNGNN*	88.23 ± 1.19	76.63 ± 0.75	89.02 ± 0.44	70.52 ± 0.74	72.84 ± 0.52	36.47 ± 0.79	43.76 ± 3.31	36.97 ± 2.70	76.90 ± 1.19	65.19 ± 0.57	75.22 ± 0.36	11.2
PathMLP	88.04 ± 1.06	77.13 ± 0.73	89.24 ± 0.48	70.88 ± 0.72	76.97 ± 0.46	37.95 ± 0.73	<u>46.46 ± 5.20</u>	40.61 ± 2.31	79.65 ± 0.83	77.74 ± 0.52	<u>85.97 ± 0.20</u>	<u>5.4</u>
PathMLP+	<u>88.71 ± 0.91</u>	77.55 ± 0.92	89.75 ± 0.43	71.79 ± 0.57	76.08 ± 0.32	36.86 ± 0.79	46.74 ± 3.15	41.17 ± 3.00	84.25 ± 1.08	79.36 ± 0.46	86.18 ± 0.24	3.5

Table 2: Node classification results on real-world benchmarks (Anomaly Group). Boldface letters are used to mark the best results while underlined letters are used to mark the second best results. † represent the homophily is evaluated by adjusted homophily.

	Chameleon	Squirrel	Questions	Amazon-ratings	BGP	Texas	Cornell	Wisconsin	NBA	Avg. Rank
Homophily	0.23	0.22	0.02†	0.38	0.25	0.09	0.12	0.19	0.40	
#Nodes	2277	5201	48921	24492	63977	183	183	251	403	
#Edges	62792	396846	307080	186100	673866	574	557	916	21645	
#Features	2325	2089	301	300	287	1703	1703	1703	95	
#Classes	5	5	2	5	8	5	5	5	2	
MLP	49.76 ± 2.74	31.85 ± 1.44	54.08 ± 3.13	45.29 ± 0.56	65.20 ± 0.68	83.89 ± 4.50	<u>79.68 ± 4.80</u>	88.02 ± 4.64	52.22 ± 8.61	10.4
GCN	66.46 ± 2.89	46.31 ± 2.61	64.22 ± 1.36	47.52 ± 0.56	61.42 ± 0.81	61.67 ± 5.83	56.94 ± 5.44	61.76 ± 5.00	72.22 ± 5.46	11.6
GraphSAGE	65.87 ± 3.01	47.80 ± 2.20	75.46 ± 1.19	49.20 ± 0.60	65.74 ± 0.81	83.33 ± 4.72	77.78 ± 4.90	87.25 ± 3.95	72.22 ± 4.44	6.8
GAT	66.42 ± 2.72	47.99 ± 2.58	76.43 ± 0.98	48.55 ± 0.76	64.64 ± 0.81	57.78 ± 8.26	53.33 ± 4.50	61.76 ± 4.16	65.87 ± 8.57	10.6
GPRGNN	66.29 ± 2.64	47.08 ± 1.42	59.55 ± 2.39	48.19 ± 0.92	64.47 ± 0.89	82.50 ± 5.08	78.89 ± 6.31	86.67 ± 4.22	70.16 ± 5.28	10.0
H2GCN*	54.66 ± 2.31	34.02 ± 1.20	75.85 ± 1.41	46.31 ± 0.44	65.16 ± 0.90	83.89 ± 6.25	76.94 ± 5.56	86.86 ± 2.78	72.06 ± 5.35	9.7
RAWGNN	53.71 ± 4.43	37.44 ± 1.73	74.05 ± 0.94	47.82 ± 0.65	64.95 ± 0.71	76.11 ± 3.97	73.89 ± 7.43	82.75 ± 3.50	72.54 ± 5.65	11.2
LINKX	73.93 ± 2.94	65.88 ± 1.06	75.07 ± 1.61	<u>52.68 ± 0.44</u>	65.21 ± 0.69	68.33 ± 6.95	63.06 ± 8.29	61.18 ± 5.90	73.02 ± 4.10	7.7
GloGNN*	74.04 ± 2.92	45.73 ± 4.25	OOM	52.46 ± 0.81	OOM	81.94 ± 6.96	79.44 ± 4.57	<u>88.04 ± 2.84</u>	71.27 ± 8.07	8.0
FSGNN	65.12 ± 2.93	46.86 ± 1.45	<u>77.15 ± 1.20</u>	50.82 ± 0.76	OOM	83.89 ± 5.52	79.17 ± 7.55	87.45 ± 4.73	70.63 ± 3.68	7.1
FAGCN	58.84 ± 3.54	39.13 ± 1.72	76.39 ± 1.83	47.69 ± 0.77	65.15 ± 1.19	83.61 ± 5.31	<u>79.64 ± 6.86</u>	87.45 ± 3.48	70.48 ± 4.38	8.2
ACMGCN	68.26 ± 2.47	54.11 ± 1.28	72.78 ± 1.51	49.06 ± 0.32	65.83 ± 1.43	84.17 ± 6.55	79.44 ± 6.03	87.45 ± 3.94	70.48 ± 5.41	5.8
GCNII*	59.16 ± 2.96	43.30 ± 1.25	74.16 ± 0.76	47.98 ± 0.83	65.62 ± 1.01	<u>85.00 ± 6.44</u>	78.06 ± 4.23	86.86 ± 2.78	70.48 ± 5.25	8.6
SNGNN*	62.75 ± 2.63	34.99 ± 1.42	75.42 ± 0.72	47.35 ± 0.88	64.44 ± 1.22	64.44 ± 6.78	54.72 ± 8.39	67.06 ± 6.46	73.17 ± 4.46	11.6
PathMLP	74.40 ± 2.03	<u>66.17 ± 1.80</u>	74.50 ± 1.12	52.66 ± 0.60	<u>66.10 ± 0.67</u>	85.28 ± 5.56	79.44 ± 5.43	88.43 ± 2.84	<u>73.49 ± 5.75</u>	2.7
PathMLP+	<u>74.04 ± 2.66</u>	66.30 ± 1.63	77.21 ± 1.13	52.76 ± 0.60	66.32 ± 0.94	82.50 ± 9.17	75.28 ± 7.91	84.51 ± 2.52	74.76 ± 4.20	<u>4.2</u>

5.5 Analysis of Path Sampling

To verify the effectiveness and superiority of our path sampling strategy, we compare it with the BFS and DFS samplers provided by RAWGNN. Fig. 3 counts the average order of candidate paths for each node obtained by different path samplers on partial datasets,

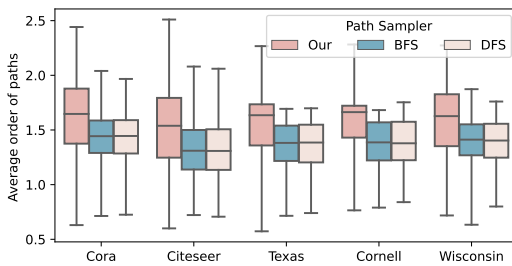
from which we can observe that: 1) our similarity-based path sampler can extract more paths with higher-order information; 2) our sampler can extract paths with a broader range of orders. Combining with Fig. 1, we can conclude that our sampler is better at capturing higher-order homophily compared to BFS and DFS.

Table 3: Impact of path sampling strategies on PathMLP.

Path Sampler	Cora	Citeseer	Pubmed	Cora-full	Actor	Chameleon-f	Squirrel-f	Tolokers	Roman-empire	Penn94	Count
Our	88.22 ± 0.46	76.32 ± 0.71	88.22 ± 0.46	70.59 ± 1.13	36.34 ± 1.02	43.65 ± 3.84	39.06 ± 2.08	78.54 ± 1.63	73.53 ± 0.30	84.80 ± 0.35	Our: 14
DFS	86.97 ± 1.12	76.51 ± 0.93	88.07 ± 0.49	70.42 ± 0.84	35.34 ± 1.02	43.59 ± 3.90	36.99 ± 2.31	78.54 ± 1.65	75.29 ± 0.42	84.79 ± 0.26	
BFS	87.30 ± 1.14	76.06 ± 0.66	88.17 ± 0.52	70.56 ± 0.93	35.27 ± 1.00	43.52 ± 3.44	38.29 ± 2.40	78.47 ± 1.64	81.28 ± 0.37	84.78 ± 0.30	
Path Sampler	Electronics	Chameleon	Squirrel	Texas	Cornell	Wisconsin	NBA	Questions	Amazon-ratings	BGP	Count
Our	76.68 ± 0.39	69.47 ± 2.51	62.41 ± 1.35	82.50 ± 3.22	78.06 ± 4.43	86.67 ± 2.23	72.38 ± 6.13	73.54 ± 1.20	51.93 ± 0.57	64.85 ± 0.99	DFS: 4
DFS	76.36 ± 0.38	69.82 ± 2.31	63.43 ± 1.53	81.94 ± 4.39	76.11 ± 5.27	86.56 ± 3.59	72.06 ± 4.44	73.15 ± 0.97	51.93 ± 0.62	65.27 ± 1.11	
BFS	76.39 ± 0.34	68.75 ± 2.07	62.79 ± 1.26	83.33 ± 6.55	74.44 ± 4.50	85.49 ± 4.05	71.11 ± 5.12	72.54 ± 0.82	51.92 ± 0.65	65.00 ± 1.08	

Table 4: Impact of path sampling strategies on PathMLP+.

Path Sampler	Cora	Citeseer	Pubmed	Cora-full	Actor	Chameleon-f	Squirrel-f	Tolokers	Roman-empire	Penn94	Count
Our	88.30 ± 1.56	76.66 ± 1.38	88.67 ± 0.41	71.38 ± 0.65	35.11 ± 1.28	44.49 ± 3.56	40.65 ± 2.17	78.49 ± 1.08	76.97 ± 0.40	84.70 ± 0.34	Our: 13
DFS	87.99 ± 0.87	76.72 ± 1.61	88.80 ± 0.66	71.10 ± 0.77	34.82 ± 0.77	43.09 ± 3.11	39.44 ± 1.73	78.76 ± 1.02	82.99 ± 0.26	84.59 ± 0.40	
BFS	87.71 ± 1.46	76.75 ± 1.49	88.60 ± 0.52	71.06 ± 0.71	34.58 ± 0.89	43.88 ± 3.97	39.21 ± 2.35	78.64 ± 0.99	78.35 ± 0.46	84.64 ± 0.29	
Path Sampler	Electronics	Chameleon	Squirrel	Texas	Cornell	Wisconsin	NBA	Questions	Amazon-ratings	BGP	Count
Our	75.76 ± 0.41	69.65 ± 2.47	62.89 ± 1.73	75.00 ± 6.80	74.44 ± 4.86	81.37 ± 3.95	72.86 ± 7.76	74.55 ± 1.66	51.99 ± 0.49	65.59 ± 0.95	DFS: 3
DFS	75.64 ± 0.47	69.62 ± 2.38	62.17 ± 1.26	76.11 ± 6.31	70.83 ± 5.44	80.39 ± 3.81	71.27 ± 5.10	68.73 ± 1.29	51.96 ± 0.60	65.51 ± 0.93	
BFS	75.70 ± 0.40	70.29 ± 1.84	63.44 ± 1.39	77.22 ± 5.04	72.50 ± 5.47	80.98 ± 2.27	71.75 ± 5.88	68.64 ± 1.36	51.91 ± 0.61	65.49 ± 1.12	

**Figure 3: Statistics of the average order of candidate paths for each node obtained by different path sampling strategies.**

Furthermore, we replace our sampler in our framework with DFS and BFS respectively, and conduct comparison experiments on all datasets. Table 3 and Table 4 illustrate the impact of different sampling strategies on PathMLP and its variant, respectively. As can be seen, our sampling strategy aids the models in achieving the best performance on most datasets, suggesting that our sampler can relatively acquire more helpful high-order homophily information, while also demonstrating better versatility. The other two samplers only perform well on a small portion of the datasets, displaying limited versatility.

5.6 Parameter Analysis

We further investigate the effect of two important hyper-parameters, i.e., the path length $d + 1$ and the number of paths N , on the performance of our methods. We make d vary in $\{3, 4, 5, 6, 7\}$ and make N vary in $\{2, 4, 6, 8, 10, 12, 15, 18\}$. Fig. 4 shows the performance variation of PathMLP with different combinations of hyper-parameters, from which it can be observed that: 1) on the homophilous dataset *Cora*, better performance is obtained by using shorter paths; 2) on the heterophilous datasets *Chameleon-f* and *Wisconsin*, better performance is obtained by using longer paths. These phenomena are

consistent with our intuition that on homophilous graphs, shorter paths are sufficient to capture rich low-order homophily information, while on heterophilous graphs, longer paths are needed to capture more high-order information. Moreover, the impact of the number of paths on the model does not show a clear pattern.

5.7 Efficiency Analysis

To compare the computational efficiency of our methods and baselines (especially path-based methods), we perform efficiency analysis experiments on *Pubmed*. For path-based methods (PathMLP, PathMLP+, RAWGNN), we set the number of paths used per node to $N = 12$ and the path length to $d + 1 = 4$. Fig. 5 shows the average running time of all methods for each epoch, from which we can see that our methods have about 11.8 times efficiency improvement relative to RAWGNN, and this improvement grows as the number of paths (N) increases. This phenomenon indicates that our methods using MLP to encode path features is much more computationally efficient than these methods using RNN-like models (RAWGNN, PathNet). In addition, our methods is close to GloGNN++, FSGNN, ACMGCN, GPRGNN and lower than SNGNN+ in terms of computational efficiency. In summary, PathMLP exhibits relatively high computational efficiency.

5.8 Over-smoothing Analysis

To verify that our method is immune to the over-smoothing problem, we conduct model depth experiments on four datasets. Specifically, we compare classical methods (GCN, GAT) and high-order methods (H2GNN), which obtain high-order information through stacking, while our method obtains high-order information by increasing path length. Fig. 6 shows the performance of all methods at different model depths (path lengths). As can be seen, the performance of classical GNNs rapidly decrease with increasing model depth, showing a significant over-smoothing phenomenon. For H2GCN, as the model depth increases from 2 layers to 8 layers, the

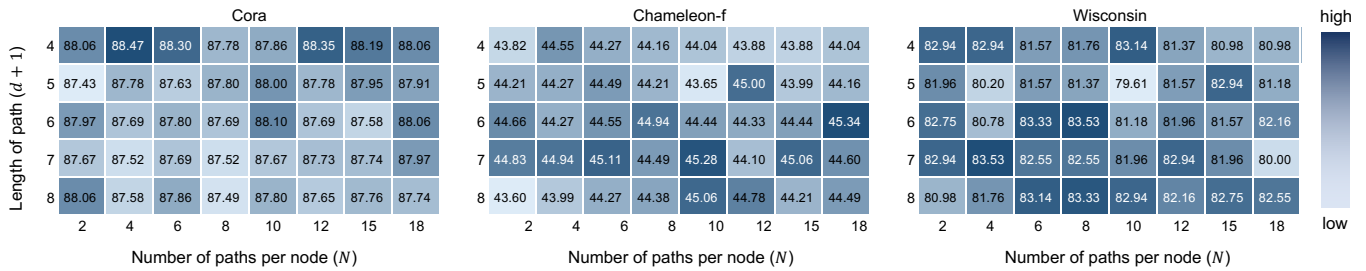


Figure 4: Impact of hyper-parameters in PathMLP+.

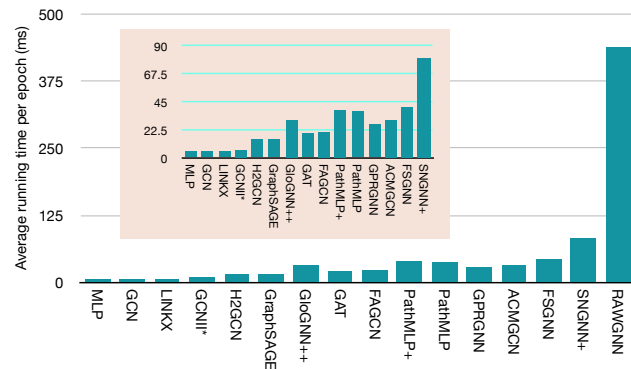


Figure 5: Average running time per epoch (ms).

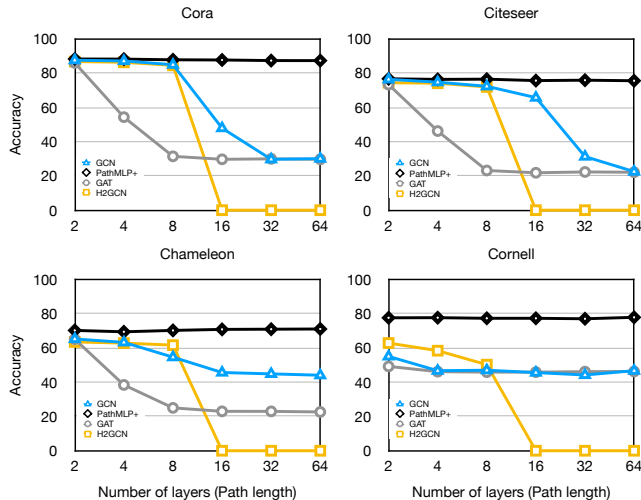


Figure 6: The performance of GNNs with increasing model depths (or path length).

performance declines gradually, hinting at the suspicion of falling into over-smoothing. When the model depth exceeds 16 layers, memory overflow occurs in the model. In contrast, our method shows stable performance with increasing path length, indicating its immunity to the over-smoothing problem.

6 CONCLUSION

To obtain high-order homophily on heterophilous graphs, we propose a path sampling strategy based on feature similarity. This paves a way for a lightweight model named PathMLP, which can encode messages carried by paths via simple transformation and concatenation operations, and effectively learn node representations. Experiments demonstrate that our path sampling strategy is able to obtain higher-order information, effectively avoiding the over-smoothing problem caused by layer stacking. Meanwhile, all feature extraction, propagation, aggregation, and transformation are implemented through MLP only, making PathMLP highly computationally efficient. Finally, our methods achieves SOTA on 16 out of 20 real-world datasets, underlining its generality across datasets.

A DETAILS OF DATASETS

A.1 Normal Group

- **Cora, Citeseer and Pubmed** [28] are homophily literature citation network datasets which nodes represent papers and edges represent the citation relationship between papers. Node features are the bag-of-words which describe whether each word exists in the paper, and node label denotes the academic topic.
- **Cora-full** [4, 29] contains more papers and academic topics. The definition of nodes, edges and node features are same as Cora.
- **Actor** [31] is a heterophily actor subgraph in co-occurrence network. Each node represents an actor and edge denotes co-occurrence on the same Wikipedia page. The graph utilizes some keywords in the Wikipedia pages as node features.
- **Chameleon-f and Squirrel-f** [26] are obtained by de-duplication operations on Chameleon and Squirrel.
- **Tolokers** [26] is a social network from Toloka crowdsourcing platform. Nodes represent workers and edges will be connected if tolokers works on same task. Node features include the worker’s profile information and task performance statistics. The label denotes whether the worker is banned in one project.
- **Roman-empire** [26] is constructed by the Roman Empire article from Wikipedia. Each node is a word of the article and edges are based on dependency of words. The method of FastText extracts the embeddings of words. And the node is classified by its syntactic role.
- **Penn94** [17] is a friendship social network from Facebook. Each node represents a student and is labeled with the gender of user.

Edges represent the relationship of students. Node features consist of basic information about student which are major, second major/minor, dorm/house, year and high school.

- **Electronics** [22] is a network of amazon product. Nodes represent the product of Electronics and edges represent the association of various products. The dataset classifies electronic products into 167 categories, while node features represent product information.

A.2 Anomaly Group

- **Chameleon and Squirrel** [17] are Wikipedia page-page networks which nodes represent articles and edges represent links of nodes. Node features are indicated by nouns in article.
- **Texas, Cornell and Wisconsin** [24] are heterophily webpage datasets which nodes represent webpages and edges represent hyperlinks. Node features are the bag-of-words and node labels are pages categories.
- **NBA** [8] is a social network about NBA basketball players. Each node represent a NBA basketball players and edges denote the relationship of these basketball players. The statistics information of players consist of node features and the players are divided into U.S. players and oversea players.
- **Questions** [26] collect the question-answering data from website Yandex Q. Nodes indicate users and edges represent the link relationship of two users. Questions use FastText embeddings to describe node features. The label denotes whether users remain active on the website.
- **Amazon-ratings** [26] is a amazon co-purchasing network. Nodes are products and edges connect the nodes which are frequently bought together. The dataset utilize FastText embeddings to describe node features like Questions. The task is to predict the rating values for products in five classes.
- **BGP** [20] is a Border Gateway Protocol Network. The BGP network consists of many router nodes, which are connected by BGP sessions.

A.3 Data Leakage Detection

Here, we design simple methods to detect and verify data leakage. Specifically, for the detection experiments, we first concatenate the adjacency matrix A and label matrix Y , then check for the duplication rate of each vector ($A_i \parallel Y_i$). For the verification experiment, we design a two-layer MLP, incorporating features from a mapped adjacency matrix after the first layer, similar to LINKX. If its performance significantly surpasses that of the MLP, it is likely that the model is utilizing topological information for matching rather than node features, i.e., it has learned shortcuts. We detect and verify all datasets, with results displayed in Table 5.

B DETAILS OF HYPER-PARAMETERS

B.1 PathMLP and PathMLP+

For the transformation dimension f' of MLP_1 , we search in $\{12, 24, 32\}$ to avoid the dimensional explosion problem introduced by node feature concatenation. For the number of paths N introduced to preventing information over-squashing, we search in $\{2, 4, 6, 8, 10, 12, 15, 18\}$. For the path length parameter d , we search in $\{3, 4, 5\}$, corresponding to path lengths of $d + 1 = \{4, 5, 6\}$, respectively.

Table 5: Results for detecting and verifying data leakage. The top two rows represent the results of duplication rate detection, while the bottom three rows display the results of the verification experiment (accuracy \pm standard deviation) and performance gain.

	Chameleon	Squirrel	Questions	Amazon-ratings	BGP
A	46.29%	36.42%	42.69%	16.50%	44.86%
A + Y	46.03%	36.28%	42.06%	15.69%	43.03%
MLP	48.31 \pm 3.69	30.55 \pm 0.98	50.92 \pm 1.48	44.19 \pm 0.61	64.41 \pm 0.83
MLP+A	73.56 \pm 3.05	65.68 \pm 1.48	72.18 \pm 1.27	52.65 \pm 0.48	64.91 \pm 0.60
gain	52.26% \uparrow	114.99% \uparrow	41.75% \uparrow	19.14% \uparrow	0.77% \uparrow

For the balance coefficient between node features and topological information, we search in $\{0, 0.3, 0.5\}$, where 0 means no topological information is used. The search spaces for all parameters are summarized as follows:

- **transformation dimension** f' : $\{12, 24, 32\}$;
- **number of paths** N : $\{2, 4, 6, 8, 10, 12, 15, 18\}$;
- **length parameter of path** d : $\{3, 4, 5\}$;
- **balance coefficient** β : $\{0, 0.3, 0.5\}$;
- **augmentation index** m : $\{1, 2\}$;

B.2 Baselines

We also use the NNI (Neural Network Intelligence) tuning tool in baselines with the same settings as our methods except for the specific hyper-parameters of baselines. The search spaces for specific hyper-parameter are as follow:

- **FAGCN**: $\epsilon \in \{0.2, 0.3, 0.4, 0.5\}$;
- **GPRGNN**: $K \in \{10\}$, dropout $\in \{0.5\}$, $\alpha \in \{0.5\}$, Init $\in \{PPR\}$;
- **ACMGCN**: variant $\in \{False\}$, is_need_struct $\in \{False\}$;
- **GCNII***: $\alpha \in \{0.5\}$, $\lambda \in \{0.5\}$, variant $\in \{True\}$;
- **H2GCN-1**: num_layers $\in \{1\}$, num_mlp_layers $\in \{1\}$;
- **FSGNN**: aggregator $\in \{cat, sum\}$;
- **GloGNN++**: norm_layers $\in \{1, 2, 3\}$, orders $\in \{2, 3, 4\}$, $\alpha \in \{0.0, 1.0\}$, $\beta \in \{0.1, 1.0, 0.05, 800, 1000\}$, $\gamma \in \{0, 0.1, 0.2, 0.3, 0.4, 0.5, 0.7, 0.8, 0.9\}$, $\delta \in \{0, 0.9, 1.0\}$;
- **SNGNN+**: $k \in \{1, 2, 5, 10, 30, 50\}$, num_layers $\in \{1, 2\}$, $\theta \in \{0.99, 0.9, 0.8, 0.5, 0.0, -0.5, -1.0\}$.

B.3 Common Hyper-parameter for All Methods

To make a relatively fair comparison, we set the common hyper-parameter search space of all methods to be consistent.

- **learning rate**: $\{0.005, 0.01, 0.05, 0.1\}$;
- **weight decay**: $\{5e-5, 1e-5, 5e-4, 1e-4, 5e-3\}$;
- **dropout**: $\{0.1, 0.3, 0.5, 0.7, 0.9\}$;
- **hidden dimension** f_h : $\{64\}$;

REFERENCES

- [1] Sami Abu-El-Hajja, Bryan Perozzi, Amol Kapoor, Nazanin Alipourfard, Kristina Lerman, Hrayr Harutyunyan, Greg Ver Steeg, and Aram Galstyan. 2019. Mixhop: Higher-order graph convolutional architectures via sparsified neighborhood mixing. In *International conference on machine learning*.
- [2] Uri Alon and Eran Yahav. 2021. On the Bottleneck of Graph Neural Networks and its Practical Implications. In *International Conference on Learning Representations*.

- [3] Deyu Bo, Xiao Wang, Chuan Shi, and Huawei Shen. 2021. Beyond low-frequency information in graph convolutional networks. In *Proceedings of the AAAI Conference on Artificial Intelligence*, Vol. 35. 3950–3957.
- [4] Aleksandar Bojchevski and Stephan Günnemann. 2018. Deep Gaussian Embedding of Graphs: Unsupervised Inductive Learning via Ranking. In *International Conference on Learning Representations*, 1–13.
- [5] Lutz Bornmann and Hans-Dieter Daniel. 2008. What do citation counts measure? A review of studies on citing behavior. *Journal of documentation* (2008).
- [6] Ming Chen, Zhewei Wei, Zengfeng Huang, Bolin Ding, and Yaliang Li. 2020. Simple and deep graph convolutional networks. In *International conference on machine learning*. PMLR, 1725–1735.
- [7] Eli Chien, Jianhao Peng, Pan Li, and Olga Milenkovic. 2021. Adaptive Universal Generalized PageRank Graph Neural Network. In *International Conference on Learning Representations*.
- [8] Enyan Dai and Suhang Wang. 2021. Say no to the discrimination: Learning fair graph neural networks with limited sensitive attribute information. In *Proceedings of the ACM International Conference on Web Search and Data Mining*, 680–688.
- [9] Wenqi Fan, Yao Ma, Qing Li, Yuan He, Eric Zhao, Jiliang Tang, and Dawei Yin. 2019. Graph neural networks for social recommendation. In *The world wide web conference*, 417–426.
- [10] Shengbo Gong, Jiajun Zhou, Chenxuan Xie, and Qi Xuan. 2023. Neighborhood Homophily-Guided Graph Convolutional Network. *arXiv preprint arXiv:2301.09851* (2023).
- [11] Aditya Grover and Jure Leskovec. 2016. node2vec: Scalable feature learning for networks. In *Proceedings of the 22nd ACM SIGKDD international conference on Knowledge discovery and data mining*, 855–864.
- [12] Will Hamilton, Zhitao Ying, and Jure Leskovec. 2017. Inductive representation learning on large graphs. In *Advances in neural information processing systems*, Vol. 30.
- [13] Di Jin, Rui Wang, Meng Ge, Dongxiao He, Xiang Li, Wei Lin, and Weixiong Zhang. 2022. RAW-GNN: RANdom Walk Aggregation based Graph Neural Network. In *International Joint Conference on Artificial Intelligence, IJCAI 2022*, 2108–2114.
- [14] Thomas N Kipf and Max Welling. 2017. Semi-Supervised Classification with Graph Convolutional Networks. In *International Conference on Learning Representations*.
- [15] Qimai Li, Zhichao Han, and Xiao-Ming Wu. 2018. Deeper insights into graph convolutional networks for semi-supervised learning. In *Proceedings of the AAAI conference on artificial intelligence*, Vol. 32.
- [16] Xiang Li, Renyu Zhu, Yao Cheng, Caihua Shan, Siqiang Luo, Dongsheng Li, and Weining Qian. 2022. Finding global homophily in graph neural networks when meeting heterophily. In *International Conference on Machine Learning*. PMLR, 13242–13256.
- [17] Derek Lim, Felix Hohne, Xiuyu Li, Sijia Linda Huang, Vaishnavi Gupta, Omkar Bhalerao, and Ser Nam Lim. 2021. Large scale learning on non-homophilous graphs: New benchmarks and strong simple methods. In *Advances in Neural Information Processing Systems*, Vol. 34. 20887–20902.
- [18] Ziqi Liu, Chaochao Chen, Longfei Li, Jun Zhou, Xiaolong Li, Le Song, and Yuan Qi. 2019. Geniepath: Graph neural networks with adaptive receptive paths. In *Proceedings of the AAAI Conference on Artificial Intelligence*, Vol. 33. 4424–4431.
- [19] Sitao Luan, Chenqing Hua, Qincheng Lu, Jiaqi Zhu, Mingde Zhao, Shuyuan Zhang, Xiao-Wen Chang, and Doina Precup. 2022. Revisiting Heterophily For Graph Neural Networks. In *Advances in Neural Information Processing Systems*.
- [20] Matthew Luckie, Bradley Huffaker, Amogh Dhamdhere, Vasileios Giotsas, and KC Claffy. 2013. AS relationships, customer cones, and validation. In *Proceedings of the conference on Internet measurement conference*, 243–256.
- [21] Sunil Kumar Maurya, Xin Liu, and Tsuyoshi Murata. 2022. Simplifying approach to node classification in Graph Neural Networks. *Journal of Computational Science* 62 (2022), 101695.
- [22] Julian McAuley, Rahul Pandey, and Jure Leskovec. 2015. Inferring networks of substitutable and complementary products. In *Proceedings of the ACM SIGKDD international conference on knowledge discovery and data mining*, 785–794.
- [23] Mark Newman. 2018. *Networks*. Oxford university press.
- [24] Hongbin Pei, Bingzhe Wei, Kevin Chen-Chuan Chang, Yu Lei, and Bo Yang. 2019. Geom-GCN: Geometric Graph Convolutional Networks. In *International Conference on Learning Representations*.
- [25] Oleg Platonov, Denis Kuznedelev, Artem Babenko, and Liudmila Prokhorenkova. 2022. Characterizing graph datasets for node classification: Beyond homophily-heterophily dichotomy. *arXiv preprint arXiv:2209.06177* (2022).
- [26] Oleg Platonov, Denis Kuznedelev, Michael Diskin, Artem Babenko, and Liudmila Prokhorenkova. 2023. A critical look at the evaluation of GNNs under heterophily: are we really making progress? *International Conference on Learning Representations*.
- [27] Frank Rosenblatt. 1958. The perceptron: a probabilistic model for information storage and organization in the brain. *Psychological review* 65, 6 (1958), 386.
- [28] Prithviraj Sen, Galileo Namata, Mustafa Bilgic, Lise Getoor, Brian Gallagher, and Tina Eliassi-Rad. 2008. Collective classification in network data. *AI magazine* 29, 3 (2008), 93–93.
- [29] Oleksandr Shchur, Maximilian Mumme, Aleksandar Bojchevski, and Stephan Günnemann. 2018. Pitfalls of graph neural network evaluation. *arXiv preprint arXiv:1811.05868* (2018).
- [30] Yifei Sun, Haoran Deng, Yang Yang, Chunping Wang, Jiarong Xu, Renhong Huang, Linfeng Cao, Yang Wang, and Lei Chen. 2022. Beyond Homophily: Structure-aware Path Aggregation Graph Neural Network. In *Proceedings of the Thirty-First International Joint Conference on Artificial Intelligence, IJCAI-22*. International Joint Conferences on Artificial Intelligence Organization, 2233–2240.
- [31] Jie Tang, Jimeng Sun, Chi Wang, and Zi Yang. 2009. Social influence analysis in large-scale networks. In *Proceedings of the ACM SIGKDD international conference on Knowledge discovery and data mining*, 807–816.
- [32] Kiran K Thekumparampil, Chong Wang, Sewoong Oh, and Li-Jia Li. 2018. Attention-based graph neural network for semi-supervised learning. *arXiv preprint arXiv:1803.03735* (2018).
- [33] Petar Veličković, Guillem Cucurull, Arantxa Casanova, Adriana Romero, Pietro Liò, and Yoshua Bengio. 2018. Graph Attention Networks. In *International Conference on Learning Representations*.
- [34] Felix Wu, Amauri Souza, Tianyi Zhang, Christopher Fifty, Tao Yu, and Kilian Weinberger. 2019. Simplifying graph convolutional networks. In *International conference on machine learning*, 6861–6871.
- [35] Shiwen Wu, Fei Sun, Wentao Zhang, Xu Xie, and Bin Cui. 2022. Graph neural networks in recommender systems: a survey. *Comput. Surveys* 55, 5 (2022), 1–37.
- [36] Yujun Yan, Milad Hashemi, Kevin Swersky, Yaoqing Yang, and Danai Koutra. 2022. Two sides of the same coin: Heterophily and oversmoothing in graph convolutional neural networks. In *IEEE International Conference on Data Mining*. IEEE, 1287–1292.
- [37] Yiding Yang, Xinchao Wang, Mingli Song, Junsong Yuan, and Dacheng Tao. 2021. Spagan: Shortest path graph attention network. *arXiv preprint arXiv:2101.03464* (2021).
- [38] Qiwei Zhong, Yang Liu, Xiang Ao, Binbin Hu, Jinghua Feng, Jiayu Tang, and Qing He. 2020. Financial defaulter detection on online credit payment via multi-view attributed heterogeneous information network. In *WWW*, 785–795.
- [39] Jiajun Zhou, Chenxuan Xie, Zhenyu Wen, Xiangyu Zhao, and Qi Xuan. 2022. Data Augmentation on Graphs: A Survey. *arXiv preprint arXiv:2212.09970* (2022).
- [40] Jiong Zhu, Yujun Yan, Lingxiao Zhao, Mark Heimann, Leman Akoglu, and Danai Koutra. 2020. Beyond homophily in graph neural networks: Current limitations and effective designs. In *Advances in Neural Information Processing Systems*, Vol. 33. 7793–7804.
- [41] Minhao Zou, Zhongxue Gan, Ruizhi Cao, Chun Guan, and Siyang Leng. 2023. Similarity-navigated graph neural networks for node classification. *Information Sciences* 633 (2023), 41–69.